

Enhancing Firefighter Situational Awareness in Wildland Fires

EREE 2020, Fire Protection Engineering

Kaitlyn Fichtner

Computer Science

Worcester Polytechnic Institute

Worcester, MA

kofichtner@wpi.edu

Abstract—This project focuses on improving camera-based fire detection methods with color photography, near infrared photography, and stereo vision. The detection methods are for future use in a low cost, lightweight fire detection device.

I. INTRODUCTION

In recent years wildfires are becoming more frequent in the United States [1]. The specific safety concern that this project addresses is entrapment. Entrapment is when escape routes or safety zones unexpectedly become blocked by fire [2]. This can occur when firebrands ignite spot fires outside the firefighters field of view. The spot fires can spread or a distant advancing fire front may change its course, blocking the firefighter's means of escape. While entrapment deaths per year are low, there are a small number of fires with high levels of entrapment fatalities [3]. For example, at the South Canyon fire, 14 firefighters were killed during entrapment [3]. The goal of this research project is to develop a lightweight and affordable device for detecting firebrands and spot fires. The device could enhance firefighter situational awareness as a bodycam worn by firefighters, a small handheld device, or a device attached to fire service vehicles or placed around communities at high risk of wildfires [1]. The fire detection method may also have future applications in robotics or unmanned aerial vehicles.

This report compares different methods of fire detection using both traditional color photography and near infrared (NIR) photography. It also evaluates the effectiveness of stereo vision for measuring the distance away from the camera and area of fires.

II. METHODOLOGY

A. Materials

- StereoPi
- 2 Raspberry Pi Camera Modules V2
- Raspberry Pi PiNoir Camera Module V2
- 5mm Optical Cast Plastic IR Longpass Filter
- Power Supply
- WiFi adaptor or wired internet connection
- Phone camera
- Access to fire

B. Procedure

Color Images

Color images are taken with a phone camera at a resolution of 3024 by 4032 pixels. First, auto-adjustment settings such as auto-exposure and auto-white balance are turned off. Next, the camera is placed in a stationary position facing the fire. A set of images is taken at varying ISO settings and exposure settings. Another set of images is taken at the default exposure and ISO setting. All the images are then converted to TIFF files with 16-bit color depth.

The images taken at various exposure and ISO settings are used to determine a threshold for oversaturation. Since oversaturated images produce inconsistent fire detection results, it is important to discard any images with intensities above the oversaturation threshold. The set of images taken at default settings is used to optimize and evaluate the red to green (R/G) color ratio method of fire detection.

Stereo Vision

The hardware configuration for stereo vision is shown below in *Figure 1*.

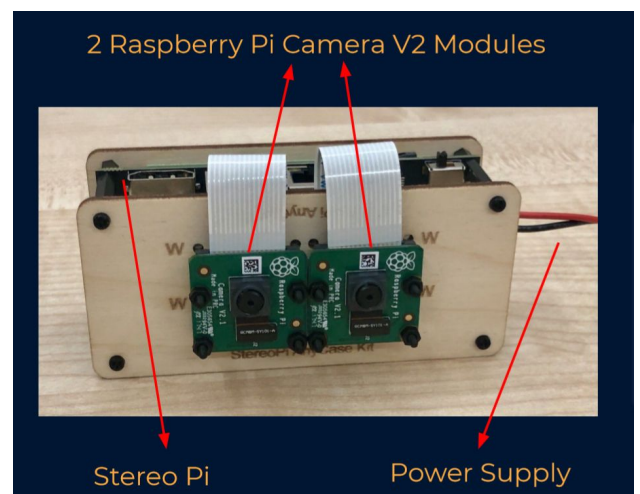


Figure 1: Hardware configuration for stereo vision

Sets of images are taken with the two cameras at 2.56 inches apart and 4.75 inches apart at a resolution of 1440 by 1920 pixels. In the image sets a folder is placed at different distances away from the camera. The folder will be used to test distance and area calculations using the stereo camera. A new camera calibration must be conducted for each time the base offset between cameras or resolution is changed. To calibrate the cameras, take a series of about 30 images holding a checkerboard at varying positions and orientations. Using the Python StereoVision package, identify the checkerboard corners, calculate reprojection errors, and export camera parameters.

With the camera parameters, produce a rectified image of each image so the left and right images are projected along the same plane. Using the rectified images, disparity is mapped between the left and right images. Disparity is the difference in X coordinates between an object in the left image and the right image: $d = X_{\text{left}} - X_{\text{right}}$. The disparity values of the pixels of the target object (the folder) are used to calculate the distance from the object to the camera.

To calculate the area of an object, create a bounding box around the pixels of the object. Next, use the distance measurement to generate the world coordinates of 2 diagonal corners of the bounding box. With 2 sets of world coordinates area can be calculated as $A = \text{base} * \text{height} = (X_2 - X_1) * (Y_2 - Y_1)$.

Near IR Images

The hardware configuration for NIR photography is shown below in *Figure 2*. Both a regular Raspberry Pi Camera Module and a PiNoir Camera Module are used so visible light intensity values and NIR intensity values can be used for detecting fire pixels. The cameras are placed as closely together as possible so that pixel coordinates of the fire are almost identical between the two images.

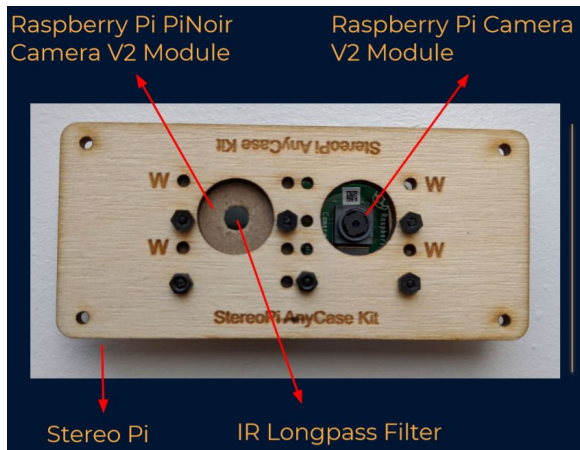


Figure 2: Hardware configuration for near IR photography

Sets of images are taken from varying perspectives and distances away from the fire. Images taken far away from the fire can be used to simulate detecting a smaller fire.

Convolutional Neural Network

Using the “FIRE dataset”, the color ratio method is applied to enhance performance of a convolutional neural network for detecting fire. A model containing only dense layers is tested against a model with multiple convolutional layers. The models are also tested using R/G color ratio binary images, grayscale images, and RGB images as inputs.

III. RESULTS

A. Color Images

The R/G color ratio method was successful at detecting pixels containing fire, however, it also detected many false positives from objects the same color as the fire. For example, in *Figure 3* below, pixels inside the red box are correctly identified pixels and pixels outside the red box are false positives. The falsely detected objects were two orange umbrellas and an orange towel. Since the color of these objects was so close to the color of the fire, the color ratio method was unable to differentiate between them. To help eliminate these false positives an image subtraction method was tested.



Figure 3: RGB image of fire (left) and binary image of detected pixels (right) with fire inside of red box

The process for image subtraction starts by normalizing the intensity between two consecutive images in a set. The average background intensity of an image is computed from the pixels in a square in the bottom right corner of the image. The average of the mean background intensities between two images is taken and each image is multiplied by the average intensity divided by the mean background intensity of that image. The result of normalizing the intensity between two images is shown below in *Figure 5* where *Figure 4* shows the raw images before averaging intensities.

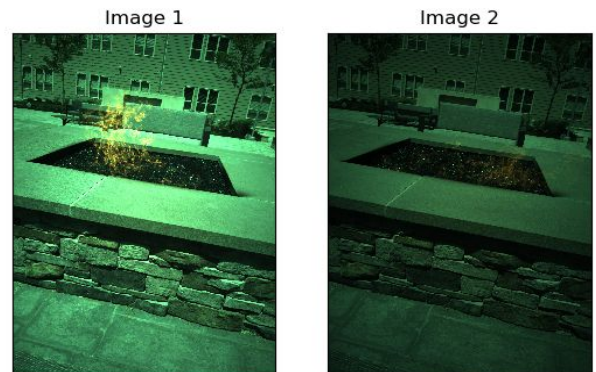


Figure 4: Raw images of two consecutive images in a set

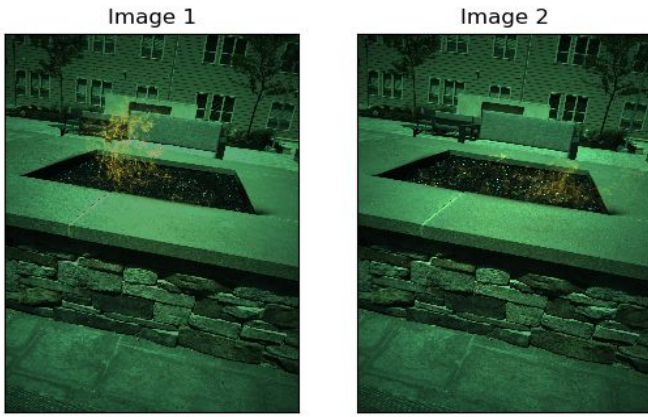


Figure 5: Images with normalized intensities

Next, one image is subtracted from the next image in the set. The pixels with a difference in intensity value below a certain threshold are set to 0 so that only pixels with larger changes in intensity are kept. The resulting image can be seen below in Figure 6.

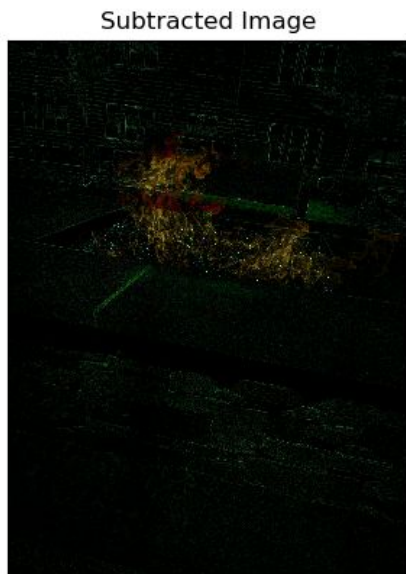


Figure 6: Subtracted image

Finally, a binary image is produced using the R/G color ratio of the pixels in the subtracted image. The resulting binary image is shown in Figure 7.



Figure 7: Binary image with detected fire pixels in yellow

The image subtraction method reduced the number of false positives detected. For example, in Figure 8, the image subtraction eliminates the false positives from the umbrellas and towel. The method also detects a larger number of pixels from the fire.

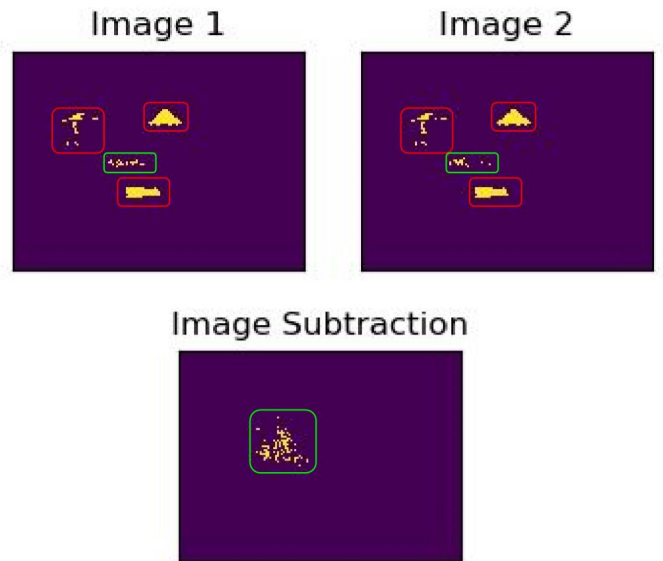


Figure 8: Binary images of two individual images (top) and binary image result of image subtraction (bottom)

B. Stereo Vision

When measuring the distance away from the camera of a folder, a distance within 25 inches of the actual distance was calculated for all images when the folder was placed less than 100 inches away from the camera. With the folder placed beyond 100 inches from the camera, distance measurements were very inaccurate. This is demonstrated in *Figure 9*, where correct distance calculations will fall on the blue line.

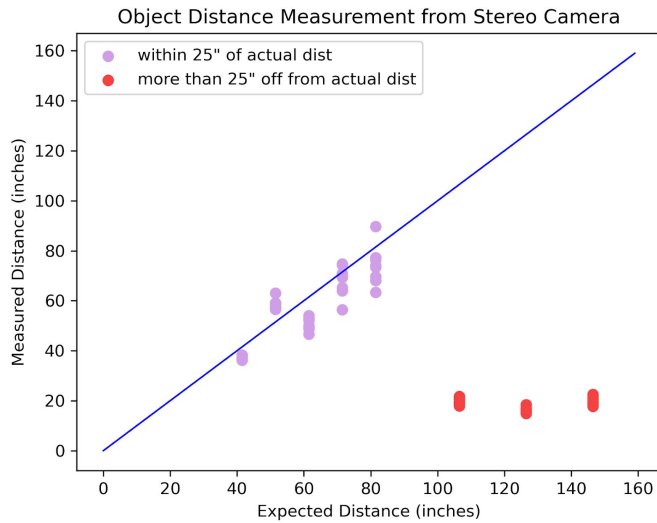


Figure 9: Actual distance vs. measured distance of a folder using stereo vision

Similarly, the area calculations were close to the actual area of the folder when the folder was less than 100 inches away from the camera. However, when the folder was beyond 100 inches away, the area calculation was thrown off by the inaccurate distance measurement used in the area calculation. The area measurements of the folder are shown in *Figure 10* below, where correct area measurements will fall along the blue line.

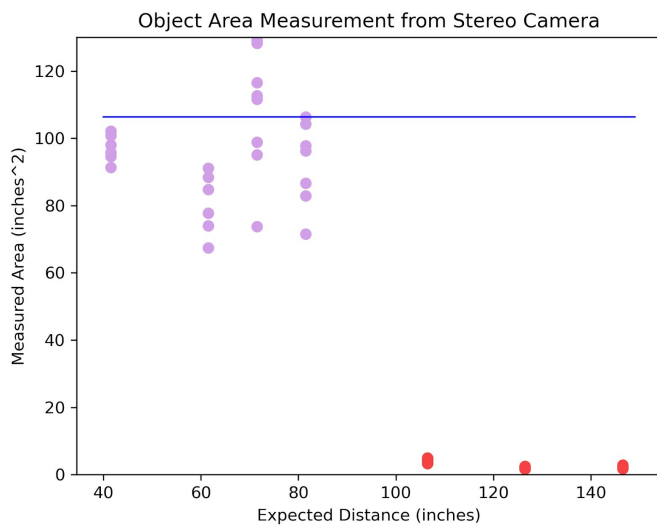


Figure 10: Actual distance vs. measured area of a folder using stereo vision

When calculating the distance from a fire to the camera, area and distance measurements were very inconsistent. As seen in *Figure 11* below, distance measurements of the fire ranged from 20 to 60 inches while the actual distance was about 60 inches for all of the images. Consequently, the area calculations were also inaccurate and varied greatly depending on the calculated distance in each image.

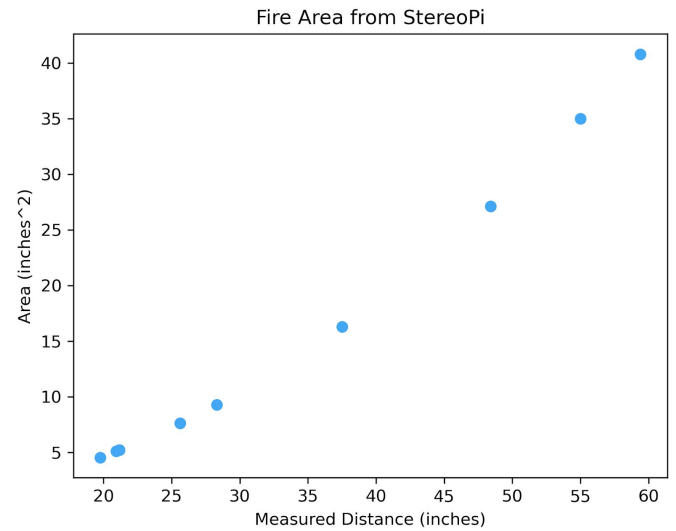


Figure 11: Measure distance vs. measured area of a fire using stereo vision

C. Near IR Images

Four methods of flame detection were tested on images from the Raspberry Pi Camera Module and the PiNoir Camera Module. The first method used only the NIR intensity values of pixels, looking for the average NIR intensity between the 3 color channels to be above a certain threshold. The second method of detection used the ratio of NIR intensity from the NIR images to red intensity from the color images (NIR/R). The third method used the ratio of red to green intensity from the color images. The fourth method combines the pixels from the other three methods using an 'OR' logical operation, keeping all pixels from any of the other methods. A visual of the color ratios alongside the raw images is shown in Figure 12.

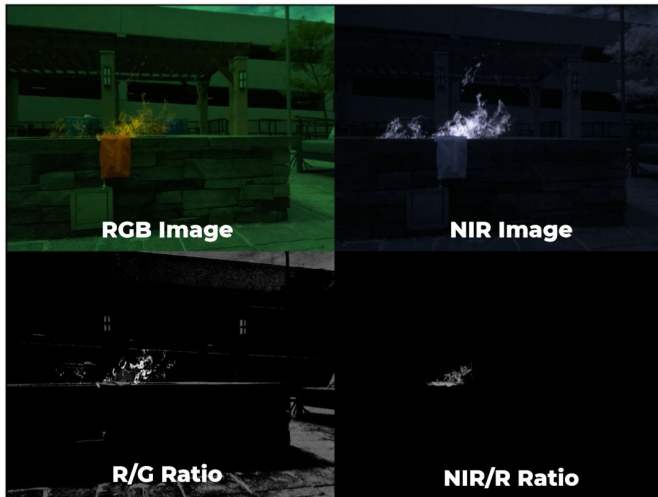


Figure 12: Raw RGB image (top left), raw NIR image (top right), R/G ratio (bottom left), and NIR.R ratio (bottom right)

The accuracy, sensitivity, and precision of the four detection methods varied greatly between the different image sets. While the conditions in image sets 1 and 3 were close to ideal, many of the image sets had high numbers of false positives from reflected light and orange colored objects. In the sixth set of images, the camera was very far away from the fire and fire was only detected in a couple of the images. The combined results from all six image sets are shown in the confusion matrices in Figure 14.

	Positive	Negative	
Positive	True Positive (TP)	False Negative (FN) Type II Error	Sensitivity $\frac{TP}{(TP + FN)}$
Negative	False Positive (FP) Type I Error	True Negative (TN)	Specificity $\frac{TN}{(TN + FP)}$
	Precision $\frac{TP}{(TP + FP)}$	Negative Predictive Value $\frac{TN}{(TN + FN)}$	Accuracy $\frac{TP + TN}{(TP + TN + FP + FN)}$

Figure 13: Confusion matrix layout [5]

Method 1 - NIR Intensity				
Actual Class	Predicted Class			
		Positive	Negative	
	Positive	123	25	0.83
	Negative	108	40	0.27
		0.53	0.62	0.55
Method 2 - NIR/R Ratio				
Actual Class	Predicted Class			
		Positive	Negative	
	Positive	113	35	0.76
	Negative	40	108	0.73
		0.74	0.76	0.75
Method 3 - R/G Ratio				
Actual Class	Predicted Class			
		Positive	Negative	
	Positive	113	35	0.76
	Negative	67	81	0.55
		0.63	0.70	0.66
Method 4 - Combined Methods				
Actual Class	Predicted Class			
		Positive	Negative	
	Positive	119	29	0.80
	Negative	90	58	0.39
		0.57	0.67	0.60

Figure 14: Confusion matrices for 4 detection methods based on images from all 6 image sets

To further evaluate the R/G ratio and NIR/R ratio methods, the *Figure 15* was created. The accuracy, sensitivity, and precision of the two methods are broken down and the causes of false positives and false negatives are explained.

Image Set	1	2	3
Accuracy NIR/R (%)	92	62	98
Accuracy R/G (%)	88	73	88
Sensitivity NIR/R (%)	83	100	96
Sensitivity R/G (%)	75	100	100
Precision NIR/R (%)	100	57	100
Precision R/G (%)	100	65	81
Explanation	Cloudy day with no false positives, a few false negatives when fire becomes small	False positives caused by sunlight or light from fire reflecting off of orange towel	Not enough sunlight or reflected sunlight to cause many false positives

Figure 15a: Table of NIR/R and R/G results for image sets 1-3

Image Set	4	5	6
Accuracy NIR/R (%)	83	61	50
Accuracy R/G (%)	83	61	2
Sensitivity NIR/R (%)	100	100	0
Sensitivity R/G (%)	100	100	3
Precision NIR/R (%)	75	56	0
Precision R/G (%)	75	56	3
Explanation	False positives caused by light reflecting off brick wall directly in front of the camera	False positives from light reflecting off brick wall, camera is closer to wall than in previous set of images	Fire is very far away & can barely be detected, false positives from orange towel

Figure 15a: Table of NIR/R and R/G results for image sets 1-3

D. Convolutional Neural Network

The model shown in *Figure 16*, had the highest performance out of all models tested. The model performed best using R/G color ratio binary images as input.

Layer (type)	Output Shape	Param #
dense_255 (Dense)	(None, 2)	178804
activation_152 (Activation)	(None, 2)	0
dense_256 (Dense)	(None, 512)	1536
dense_257 (Dense)	(None, 2)	1026
activation_153 (Activation)	(None, 2)	0
Total params: 181,366		
Trainable params: 181,366		
Non-trainable params: 0		

Figure 16: Best performing model summary

This model achieved a test accuracy of 96.7% and the validation accuracy remained close to the training accuracy through all 40 epochs, as seen in *Figure 17*.

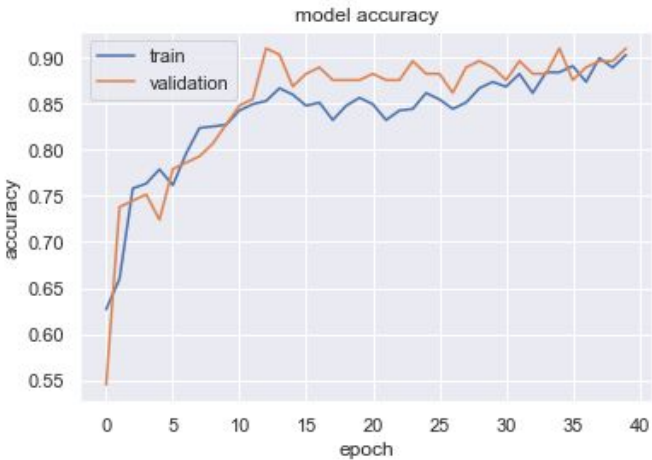


Figure 17: Model accuracy during training for best performing model with R/G color ratio inputs

The confusion matrix in *Figure 18* shows the results of evaluating the model on the test data. Out of 240 test images, 232 were correctly classified and 8 were incorrectly classified.

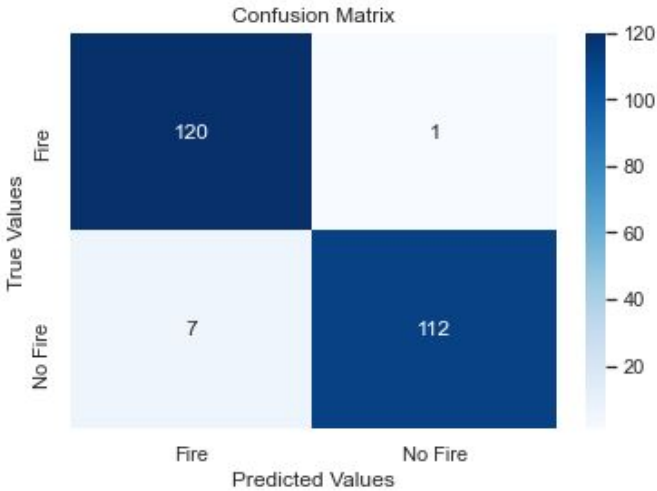


Figure 18: Confusion matrix for best performing model with R/G color ratio inputs

The performance of the model with R/G color ratio inputs performed significantly better than the same model using grayscale image inputs. The results of testing the same model with grayscale inputs resulted in a test accuracy of 72.5%, as seen in *Figure 19*.

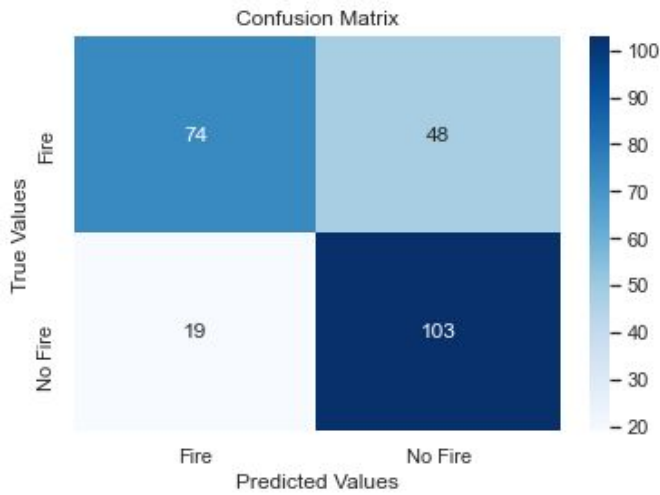


Figure 19: Confusion matrix for model with grayscale inputs

More complex models with convolutional layers were tested such as the model seen in Figure 20 and similar variations. However, none of the convolutional models tested were able to out-perform the simple model containing only dense layers.

Layer (type)	Output Shape	Param #
conv2d_11 (Conv2D)	(None, 298, 298, 128)	1664
conv2d_12 (Conv2D)	(None, 297, 297, 64)	32832
max_pooling2d_6 (MaxPooling2D)	(None, 148, 148, 64)	0
conv2d_13 (Conv2D)	(None, 147, 147, 32)	8224
max_pooling2d_7 (MaxPooling2D)	(None, 73, 73, 32)	0
flatten_3 (Flatten)	(None, 170528)	0
dense_15 (Dense)	(None, 2)	341058
Total params: 383,778		
Trainable params: 383,778		
Non-trainable params: 0		

Figure 20: Convolutional model summary

IV. DISCUSSION

A. Color Images

Image subtraction is an effective method for eliminating false positives because fire is constantly moving, while other objects in the background are stationary. However, if the false positive objects move between the two images, the false positive would still be detected in the subtracted image. For this reason, image subtraction would be less effective at eliminating false positives from something more dynamic like reflected sunlight.

B. Stereo Vision

The low resolution of the images taken with the Raspberry Pi Camera Module puts a limitation on how far away accurate distance measurements can be made from. The results showed

that objects placed beyond 100 inches away from the camera did not produce accurate disparity values or distance calculations.

Calculating the distance between a fire and the camera is extremely difficult because the fire is partially transparent. This means a disparity that is calculated for the fire, could actually be the disparity of an object behind the fire. The fire used in the test sets of images used natural gas as fuel. The natural gas produces a much more transparent fire than would be seen in a wildfire. The more solid appearance of a wildfire could be enough to make accurate disparity calculations using stereo vision.

C. Near IR Images

Out of the 4 fire detection methods tested, the NIR intensity-only method was the least successful. The NIR intensity-only method detects a large number of false positives because intensity is easily affected by factors such as exposure and brightness. Ratio methods are much more consistent even when there are changes in image brightness.

The combined method takes the best results in the true positive and false negative categories, but the worst results from the false positive and true negative categories. Because the three methods tend to already have high sensitivities and low precision, it is more important to reduce the number of false positives than it is to increase the number of true positives. The current combined method could result in an unreliable device that falsely detects fire more frequently than the NIR/R or R/G ratio methods would individually.

The NIR/R ratio and R/G ratio methods are the most consistent, but still detect false positives under certain conditions. The NIR/R method often detects false positives from reflected sunlight while the R/G ratio method detects false positives from objects with a similar color to the fire. Overall, the NIR/R ratio has a higher accuracy than the R/G ratio method.

D. Convolutional Neural Network

The convolutional neural network shows a lot of potential for improving the accuracy of the color ratio detection method. While the neural network can perform well using just the RGB color images, there are many advantages to the color ratio method. Color ratio can be used to estimate temperature, so the color ratio method can control the temperature of the fire being detected. The color ratio method also reduces the impact of the emissivity of the firebrand or soot in the flames, since it is not based on pixel intensity alone [1].

Testing this neural network on NIR images would be ideal because the NIR/R ratio performed best for locating fire pixels. A future step for this research could include developing a dataset of NIR/R images.

V. CONCLUSION

The tested fire detection methods are successful at identifying fire pixels in both color images and NIR images. However, both methods often detect false positive pixels in addition to the fire pixels. More systematic testing will need to be done to determine if the NIR/R ratio method is better than the R/G ratio method at reducing false positives. Future research should also include finding a better way to combine these two methods to reduce false positive detection and building a NIR image dataset for improving the neural network.

Because all the test images were taken in an area surrounded by buildings, the background objects and environment is very different from the setting of a wildland fire. It will be important to determine what types of false positives would be more prevalent in a wildland setting. For example, the effect of reflected sunlight could be very different in a setting with smoke in the air and fewer solid objects (like brick walls) for sunlight to reflect off of. Stereo vision should also be tested with a fire more similar to wildfire to see if a less transparent fire can produce better results.

VI. REFERENCES

- [1] Urban, J. L. *Enhancing Fire Fighter Situational Awareness in Wildland and WUI Fires*. Worcester Polytechnic Institute.
- [2] Page WG, Freeborn PH (2019) Entrapment. In: Manzello S (ed) *Encyclopedia of Wildfires and Wildland-Urban Interface (WUI) Fires*. Springer Nature
- [3] Cook J (2013) Trends in Wildland Fire Entrapment Fatalities ... Revisited
- [4] Saied, A. (2020, February 25). FIRE Dataset. Retrieved from <https://www.kaggle.com/phylake1337/fire-dataset>
- [5] Sirsat, M. (1970, January 01). Confusion Matrix. Retrieved August 01, 2020, from <https://manisha-sirsat.blogspot.com/2019/04/confusion-matrix.html>